



CHORUS

This is the accepted manuscript made available via CHORUS. The article has been published as:

# Cooperative Rearrangement Regions and Dynamical Heterogeneities in Colloidal Glasses with Attractive Versus Repulsive Interactions

Zexin Zhang, Peter J. Yunker, Piotr Habdas, and A. G. Yodh

Phys. Rev. Lett. **107**, 208303 — Published 8 November 2011

DOI: [10.1103/PhysRevLett.107.208303](https://doi.org/10.1103/PhysRevLett.107.208303)

# Cooperative rearrangement regions and dynamical heterogeneities in colloidal glasses with attractive versus repulsive interactions

Zexin Zhang,<sup>1,2,\*</sup> Peter J. Yunker,<sup>3</sup> Piotr Habdas<sup>4</sup> and A. G. Yodh<sup>3</sup>

<sup>1</sup>*Center for Soft Condensed Matter Physics and Interdisciplinary Research, Soochow University, Suzhou 215006, China,* <sup>2</sup>*Complex Assemblies of Soft Matter, CNRS-Rhodia-UPenn UMI 3254, Bristol, Pennsylvania, PA 19007, USA,* <sup>3</sup>*Department of Physics and Astronomy, University of Pennsylvania, Philadelphia, PA 19104, USA,* <sup>4</sup>*Department of Physics, Saint Joseph's University, Philadelphia, PA 19131, USA*

Water-lutidine mixtures permit the interparticle potentials of colloidal particles suspended therein to be tuned, *in situ*, from repulsive to attractive. We employ these systems to directly elucidate the effects of interparticle potential on glass dynamics in experimental samples composed of the same particles at the same packing fractions. Cooperative rearrangement regions (CRRs) and heterogeneous dynamics are observed in both types of glasses. Compared to repulsive glasses, the attractive glass dynamics are found to be heterogeneous over a wider range of time and length scales, and its CRRs involve more particles. Additionally, the CRRs are observed to be string-like structures in repulsive glasses and compact structures in attractive glasses. Thus, the experiments demonstrate explicitly that glassy dynamics depend on the sign of the interparticle interaction.

PACS numbers: 64.70.pv, 61.43.Fs, 64.70.kj, 82.70.Dd

When the temperature of a glass-forming liquid is rapidly lowered, its viscosity and relaxation times diverge due to emerging domains of particles that rearrange in a correlated manner [1]. The size and shape of these spatially clustered cooperative rearrangement regions (CRRs) are closely related to

the macroscopic properties of glasses [2, 3]. In fact, the presence of CRRs across a wide swath of disordered molecular and particulate matter has led scientists to search for universal explanations of glass formation [4-7]. Many properties of glasses, however, are predicted to depend on the details of constituent interparticle potentials [8]. For example, while repulsive colloidal glasses form when the packing fraction of repulsively interacting particles is made sufficiently large, the addition of even a small short-range attraction to particle potential in a repulsive glass can lead to the formation of so-called attractive glasses, which exhibit many new properties [9]. Exploration of the similarities and differences between glasses composed of particles with attractive versus repulsive interactions holds promise to elucidate universal aspects of the glass transition and could lead to development of new methods for manipulating properties of glassy materials [8, 9]. Unfortunately, controlled experiments that isolate the effects of interparticle interaction on glassy dynamics are rare. Even in simple attractive glasses formed by adding macromolecular depletants to dense suspensions of hard-sphere-like colloidal particles [9], for example, the addition of depletants increases background viscosity, damps particle motion, and can introduce new hydrodynamics, making direct comparisons between attractive and repulsive glasses difficult.

In this letter, we utilize a novel colloidal glass whose interparticle potential can be tuned *in situ* from short-range repulsive (producing a repulsive glass) to short-range attractive (producing an attractive glass), while other parameters such as background suspension viscosity, particle packing fraction, and particle type are held constant. The dynamical and structural behaviors of the resulting colloidal glasses are investigated by video microscopy with single-particle resolution. The experiments in both attractive and repulsive glasses indicate that structural rearrangements occur via the cooperative motion of spatially clustered particles, *i.e.*, via cooperative rearrangement regions (CRRs), a hallmark of dynamic heterogeneity [1, 3, 10]. Particles in attractive glasses, however, form long-lived bonds with

their neighbors and exhibit particle dynamics slower than those in repulsive glasses. Interestingly, our observations suggest the number of particles involved in cooperative rearrangements is larger in attractive glasses compared to repulsive glasses, the CRRs occur over a wider range of time and length scales in attractive glasses compared to repulsive glasses, and the CRRs form string-like structures in repulsive glasses and compact cluster-like structures in attractive glasses.

The glass samples consisted of a binary mixture (4:1 by number) of polystyrene spheres (nominal diameters  $\sigma_S = 1.4 \mu\text{m}$  and  $\sigma_L = 1.6 \mu\text{m}$ , Duke Scientific) to prevent crystallization [11]. The particles were suspended in a water/lutidine mixture (WL) near its critical composition (lutidine weight fraction  $c_L = 0.25$ ) and confined to a *quasi-2D* chamber between two glass coverslips (Fisher) with a spacing of  $\sim(1.1 \pm 0.05)\sigma_L$ . The chamber walls were treated with sodium hydroxide so that the particle-wall interaction was repulsive in the temperature range investigated [12]. The area fraction of the sample is calculated as,  $\phi = \left[ n_L \pi \left( \frac{\sigma_L}{2} \right)^2 + n_S \pi \left( \frac{\sigma_S}{2} \right)^2 \right] / A_T$  where  $n_L$  ( $n_S$ ) is the number of large (small) particles in the field of view, and  $A_T$  is total area of the field of view. The area fraction is tuned to 0.84, slightly below the area fraction expected for the jamming transition [13]. Video microscopy was used to collect image data for  $\sim 10^4$  seconds at a rate of 3 frames per second using a CCD camera (Sony). The field of view was  $60 \mu\text{m}$  by  $80 \mu\text{m}$  and contained approximately 3000 particles.

Colloidal particles in near-critical WL mixtures experience temperature-dependent, fluid-mediated attraction [14]. Fig. 1a shows a schematic of the WL phase diagram and experimental microscope images at two temperatures. Notice the particles are well dispersed at 300.15 K; at this temperature the particle interaction potentials are repulsive and hard-sphere-like. Increasing the temperature to 306.45 K with a microscope objective heater (Bioptechs), converts these short-range repulsions into short-range interparticle attractions, *in situ*, and the particles aggregate. We calculate the interparticle

potentials from experimentally determined pair correlation functions, measured in the dilute concentration regime using liquid structure theory [15]. In the present study, the depth of the attractive well is  $\sim 3.1k_B T$  (Fig. 1b), similar to that reported in recent investigations of attractive particle clusters in WL mixtures [16]. The particle interaction was observed to switch in an almost binary fashion from repulsive to attractive with temperature; *i.e.*, the interaction transition region of the WL mixtures was sharp compared to our temperature resolution of 0.1 K.

Both repulsive and attractive samples exhibit classic features of dynamical arrest associated with glass formation [3-7]. For example, the particle mean-square displacement (MSD) for both glass types develops a plateau initially, as particles explore “cages” created by their neighbors, and then at long times, the MSD grows again as cages rearrange [3, 4] (Fig. 1c). Notice that for any given lag-time,  $\Delta t$ , the MSD of the attractive glass is smaller than that of the repulsive glass. It has been speculated that the slower dynamics of attractive glasses are due to long-lived nearest neighbor bonds [8, 9]. This conjecture, however, has not been directly tested in real space colloidal experiments. To this end, we calculate the persistent bond parameter,  $B(\Delta t)$  [17].  $B(\Delta t)$  represents the fraction of nearest neighbor bonds at time  $t$ , identified by Delaunay triangulation, that remain unbroken across the interval  $t \rightarrow t + \Delta t$  (Fig. 1d). We see that bonds in attractive glasses are longer-lived than their repulsive glass counterparts. The long lifetime of nearest neighbor bonds in attractive glasses impedes rearrangement and slows particle dynamics, leading to smaller MSDs.

In our experiments, the area fraction and the static structure (e.g., the particle pair correlation function) of the samples do not change within measurement accuracy when the interparticle potential switches from repulsive to attractive (see *Supplementary Information*, Fig. S1). To quantify dynamic heterogeneity in attractive and repulsive glasses, the four-point susceptibility,  $\chi_4$ , is calculated as

follows [5, 6, 17, 18]. First, the two-time self-correlation function,  $Q_2(a, \Delta t)^2 = \frac{1}{N} \sum_{i=1}^N \exp\left(\frac{-\Delta r_i^2}{2a^2}\right)$ , is computed; here  $a$  is a pre-selected length scale to be probed,  $\Delta r_i^2$  is the mean squared displacement of particle  $i$  in time  $\Delta t$ , and  $N$  is the total number of particles in the sample viewing area. The four-point susceptibility quantifies the temporal fluctuations of  $Q_2$  through its variance, i.e.,  $\chi_4(a, \Delta t) = N \left( \langle Q_2(a, \Delta t)^2 \rangle - \langle Q_2(a, \Delta t) \rangle^2 \right)$ , the brackets indicate time average. The four-point susceptibility, in turn, characterizes the temporal variance of particle dynamics and is directly related to the number of particles which participate in a correlated rearrangement [17]. Here we investigate the four-point susceptibility as a function of both probing length scale,  $a$ , and time scale,  $\Delta t$ , (Fig. 2 insets) [5, 6, 18].

The susceptibilities are qualitatively and quantitatively different for the two types of glasses. For the repulsive glass (Fig. 2, inset (a)), the maximum value of  $\chi_4$  is  $\sim 20$ , whereas for the attractive glass (Fig. 2, inset (b)) this maximum is  $\sim 80$ . This observation implies that the number of particles participating in the primary cooperative rearrangements (*i.e.*, the number of particles participating in cooperative rearrangements at the “maximum” length- and time-scale) is about four times larger in glasses composed of attractive particles than in glasses composed of repulsive particles. For the attractive glass,  $\chi_4$  is large for a wide range of length-scales ( $a$ ) and lag-times ( $\Delta t$ ). Conversely, for the repulsive glass,  $\chi_4$  is only large for a relatively narrow range of  $a$  and  $\Delta t$ . In other words, attractive glass dynamics are heterogeneous over broader time and length scales than repulsive glass dynamics. If we focus on the length scales that maximize  $\chi_4$  [5, 6, 17, 18], then the four-point susceptibility displays a peaked behavior in both repulsive and attractive glasses (Fig. 2, main plot). The peak lag-times indicate the timescales over which dynamics are the most heterogeneous, and the peak heights

indicate the spatial extent of these heterogeneities. Notice, the maximum value of  $\square_4$  becomes larger and shifts towards longer lag-times when attraction is present.

To further quantify the size and shape of dynamic heterogeneities, we analyzed the spatial distribution of particles participating in cooperative rearrangements. Following previous studies [4], a cooperative rearranging region (CRR) represents a group of highly mobile particles that are nearest-neighbours. Nearest-neighbour pairings are identified using Delauney triangulation. Particles with the 10% largest displacements over a given lag-time,  $\square t$ , are defined as mobile.  $\square t$  is set to the same lag-time that maximizes  $\square_4$ , i.e., the lag-time over which dynamics are most heterogeneous [5, 6, 17, 18]. Fig. 3 shows two snapshots of repulsive and attractive glasses, wherein “fast moving” or “mobile” particles are depicted as large red spheres with arrows indicating their direction of motion; all other particles are shown as small black dots. In the repulsive glasses, the CRRs are string-like, consistent with results from theory/simulation [1-3, 10] and experiment [4-7]. Interestingly, CRRs in attractive glasses form more compact structures than those of the repulsive glass. (See the *Supplementary Information*, Fig. S2, for more snapshots.)

To quantify the morphology of CRRs, we determined the average number of nearest neighbors,  $NN$ , in the CRRs (Fig. 4a). Particles in CRRs of repulsive glasses have an average ( $\pm$  standard deviation) of  $2.5 \pm 1.0$  neighbors, reflecting their string-like structure. Particles in CRRs of attractive glasses have an average of  $4.4 \pm 1.2$  neighbors, reflecting a more compact structure. This difference in morphology is also reflected by the fractal dimension of the CRRs. To extract an estimate of this fractal dimension, the number of particles ( $N_p$ ) participating in a CRR is plotted as a function of the radius of gyration ( $R_g$ ) of the CRR, for many independent rearrangement events (see *Supplementary Information*, Fig. S3). For both types of glasses,  $N_p$  exhibits a power law dependence with  $R_g$  (Fig. 4b),

i.e.,  $N_p \sim R_g^{d_f}$ , where  $d_f$  is the fractal dimension [4, 19]. Note,  $d_f \cong 1$  for a string-like structure, and  $d_f \cong 2$  for a compact structure. In the attractive glasses,  $d_f = 1.98 \pm 0.11$ , implying that the CRRs occur in compact cluster-like regions. Conversely, in repulsive glasses  $d_f = 1.49 \pm 0.18$ , implying CRRs occur in relatively more string-like regions. Previous analytic studies [2] found that decreasing temperature increases  $d_f$ . The increased short-range attraction in our experiments is analogous to decreasing an effective temperature, and the attraction in our colloidal glasses is observed to slow particle dynamics (Fig. 1c) and increase  $d_f$  (Fig. 4). Such behavior is similar to the effect of temperature in molecular glasses; in this sense, our observations are consistent with previous theoretical studies [2].

To conclude, we have presented novel real-space experiments demonstrating that glassy dynamics, such as cooperative rearrangement regions (CRRs) and dynamical heterogeneity in colloidal glasses, is directly related to microscopic interparticle potential. Short-range attraction leads to the formation of long-lived bonds between colloidal particles, and because these bonds are difficult to break, particle dynamics are slow, and rearrangements occur less often. The experiments therefore suggest that when a rearrangement does occur, attractive bonds pull neighboring particles, causing them to participate in the rearrangement. As a result, more particles are involved in CRRs in attractive glasses, and rearrangements happen over a more diverse range of length and timescales in attractive glasses than in repulsive ones. Topologically, CRRs in attractive glasses form compact clusters, while CRRs in repulsive glasses form string-like clusters. Thus, tuning the interparticle potential offers a new way to control macroscopic properties of glasses and, possibly, their mechanical responses [20]. For example, the yielding of repulsive glass and attractive glass are different. For the former it is due to the breaking of local topological cages, for the latter the breaking of nearest-neighbor bonds produces yielding [21]. Such previous observations are consistent with the microscopic picture of dynamics found in the present study. Other rheological properties of glasses, observed in recent studies on shear thickening [22], can

also be explored using the attractive systems presented here. Finally, while the precise relationship of 2D glasses to 3D glasses is an open question, prior results from simulations and experiments suggest that dimensionality has little qualitative effect on dynamic heterogeneities and particle rearrangements [23]. The results presented here are therefore expected to be relevant for 3D and call for similar studies in 3D.

We thank Daniel Chen and Matt Lohr for discussions. Z. Z. acknowledges financial support of the National Science Foundation of China through grants 91027040, 11004143, Jiangsu Specially-Appointed Professor and PAPD program. P. H. acknowledges financial support from an award from Research Corporation. A. G. Y acknowledges financial support of the National Science Foundation through DMR-0804881, PENN MRSEC DMR-0520020, and NASA NNX08AO0G.

\* zhangzx@suda.edu.cn

- [1] G. Adam, and J. H. Gibbs, *J. Chem. Phys.* **43**, 139 (1965).
- [2] J. D. Stevenson, J. Schmalian, and P. G. Wolynes, *Nat. Phys.* **2**, 268 (2006).
- [3] M. D. Ediger, *Annual Rev. Phys. Chem.* **51**, 99 (2000).
- [4] E. R. Weeks et al., *Science* **287**, 627 (2000).
- [5] L. Berthier et al., *Science* **310**, 1797 (2005).
- [6] O. Dauchot, G. Marty, and G. Biroli, *Phys. Rev. Lett.* **95**, 265701 (2005).
- [7] K. Watanabe, and H. Tanaka, *Phys. Rev. Lett.* **100**, 158002 (2008).
- [8] F. Sciortino, *Nat. Mat.* **1**, 145 (2002); K. A. Dawson, *Current Opin. Colloid Interf. Sci.* **7**, 218 (2002); G. Foffi et al., *Phys. Rev. Lett.* **94**, 078301 (2005); R. W. Hall, and P. G. Wolynes, *J. Phys. Chem. B* **112**, 301 (2008); L. Berthier, and G. Tarjus, *Phys. Rev. Lett.* **103**, 170601 (2009).
- [9] V. Trappe et al., *Nature* **411**, 772 (2001); K. N. Pham et al., *Science* **296**, 104 (2002); T. Eckert, and E. Bartsch, *Phys. Rev. Lett.* **89**, 125701 (2002); L. J. Kaufman, and D. A. Weitz, *J. Chem. Phys.* **125**, 074716 (2006); A. Latka et al., *EPL* **86**, 58001 (2009); C. L. Klix, C. P. Royall, and H. Tanaka, *Phys. Rev. Lett.* **104**, 165702 (2010).
- [10] H. C. Andersen, *PNAS* **102**, 6686 (2005); S. C. Glotzer, *J. Non-Cryst. Solids* **274**, 342 (2000).

- [11] R. Yamamoto, and A. Onuki, Phys. Rev. E **58**, 3515 (1998); D. N. Perera, and P. Harrowell, J. Chem. Phys. **111**, 5441 (1999).
- [12] C. Hertlein et al., Nature **451**, 172 (2008).
- [13] Z. X. Zhang et al., Nature **459**, 230 (2009); P. J. Yunker et al., Phys. Rev. E **83**, 011403 (2011).
- [14] D. Beysens, and T. Narayanan, J. Statistical Phys. **95**, 997 (1999); X. H. Lu et al., Phys. Rev. Lett. **100**, 045701 (2008); D. Bonn et al., Phys. Rev. Lett. **103**, 156101 (2009).
- [15] Y. L. Han, and D. G. Grier, Phys. Rev. Lett. **91**, 038302 (2003); J. Baumgartl, and C. Bechinger, Europhys. Lett. **71**, 487 (2005).
- [16] P. J. Yunker et al., Phys. Rev. Lett. **106**, 225503 (2011).
- [17] A. R. Abate, and D. J. Durian, Phys. Rev. E **76**, 021306 (2007); A. S. Keys et al., Nat. Phys. **3**, 260 (2007).
- [18] N. Lacevic et al., J. Chem. Phys. **119**, 7372 (2003).
- [19] P. J. Lu et al., Phys. Rev. Lett. **96**, 028306 (2006).
- [20] P. Schall, D. A. Weitz, and F. Spaepen, Science **318**, 1895 (2007); A. Furukawa et al., Phys. Rev. Lett. **102**, 016001 (2009).
- [21] K. N. Pham et al., Europhys. Lett. **75**, 624 (2006). E. Zaccarelli, and W. C. K. Poon, PNAS **106**, 15203 (2009). G. Petekidis, D. Vlassopoulos, and P. N. Pusey, J. Phys.-Condens. Mat. **16**, S3955 (2004).
- [22] E. Brown and H. M. Jaeger, Phys. Rev. Lett. **103**, 086001 (2009), E. Brown et. al. Nat. Mater. **9**, 220 (2010).
- [23] L. Berthier, G. Biroli, J.-P. Bouchaud, L. Cipeletti, and W. van Saarloos, *Dynamical heterogeneities in glasses, colloids, and granular media* (Oxford University Press, 2011).

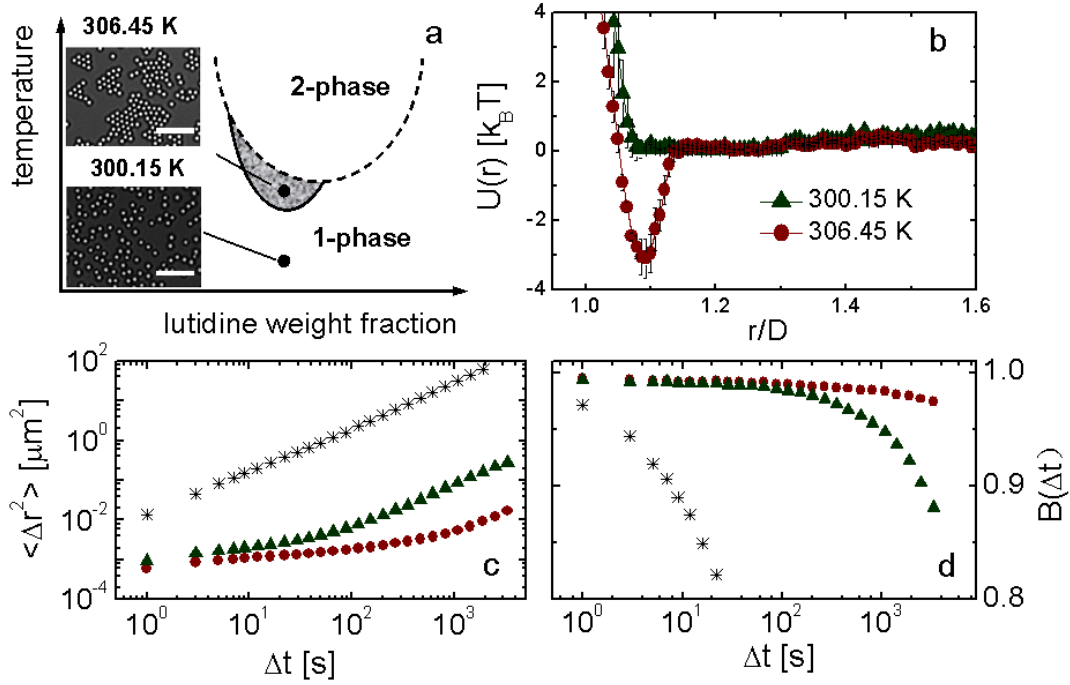


**FIG. 1.** (a) Schematic phase diagram of water and lutidine (WL) mixtures. Two samples (monodisperse polystyrene spheres,  $D = 1.4 \mu\text{m}$ ), are shown at 300.15K and 306.45 K, corresponding to the repulsively- and attractively-interacting (shaded area) regimes, respectively. At 306.45 K attraction is ‘turned on’ and particles aggregate, as evident in the bright-field microscope images (scale bars are  $10 \mu\text{m}$ ). (b) Experimentally measured interparticle potential,  $U(r)$ , for samples at 300.15K and 306.45 K, respectively. Error bars represent standard deviation. (c) Mean squared displacement of the particles,  $\langle \Delta r^2 \rangle$ , is plotted against lag-time,  $\Delta t$ , derived from colloidal liquid sample (stars,  $\phi = 0.18$ ), repulsive glass sample (triangles,  $\phi = 0.84$ ), and attractive glass sample (filled circles,  $\phi = 0.84$ ). (d) The persistent bond parameter,  $B(\Delta t)$ , plotted against lag-time  $\Delta t$ ; symbols in (d) have the same meanings as in (c).

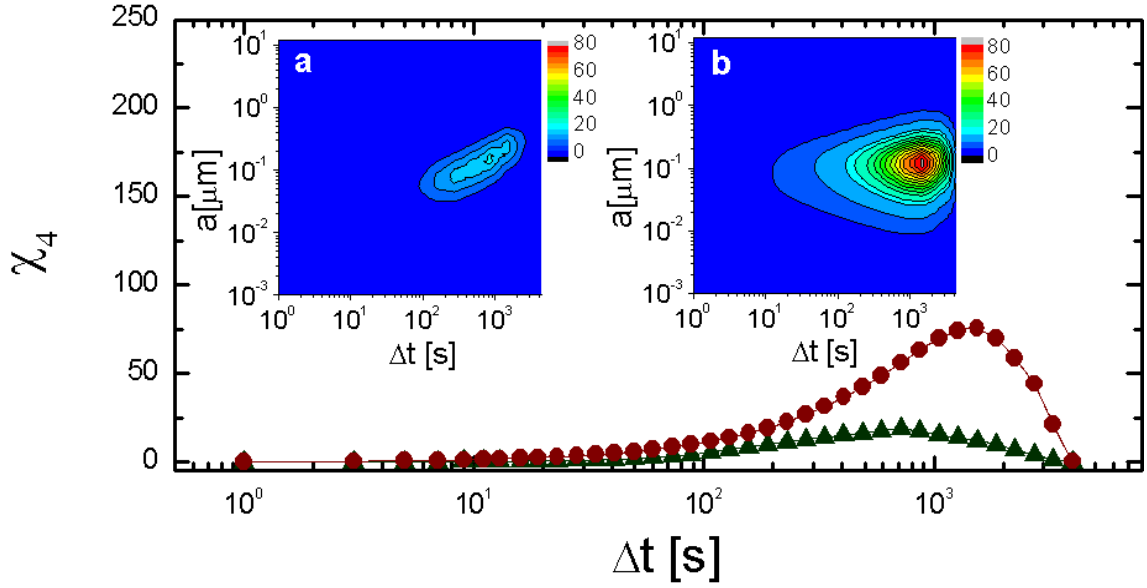


**FIG. 2.** Dynamical susceptibility,  $\chi_4$  for the repulsive (triangles) glass and the attractive glass (circles), with probing length scale,  $a$ , chosen to maximize the value of  $\chi_4$ , here  $a_1 = 0.169 \mu\text{m}$  and  $a_2 = 0.108 \mu\text{m}$  for repulsive glass and attractive glass, respectively. Insets: Dependence of  $\chi_4$  on all probing length scales,  $a$ , and time scales,  $\Delta t$ , for (a) repulsive glass and (b) attractive glass.

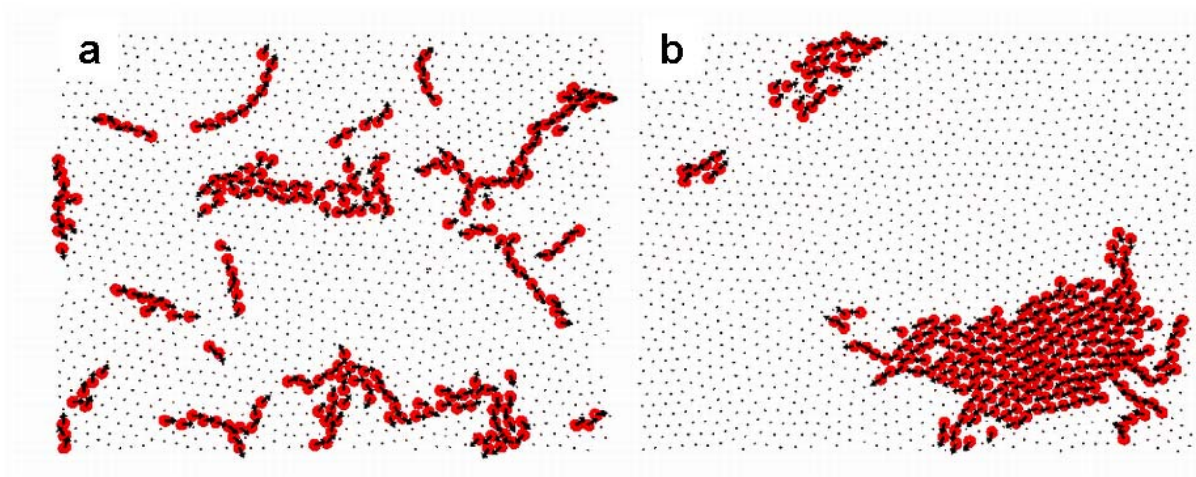


**FIG. 3.** Snapshots of cooperatively rearranging particles for repulsive glass (a) and attractive glasses (b). The red spheres are drawn to scale and represent the 10% fastest particles. The rest of particles are shown as black dots, reduced in size for clarity. Arrows indicate the direction of motion. (see *Supplementary Information*, Fig. S2, for more examples of such rearrangement events.) The time interval between images used to generate the snapshots of CRRs was set to the value that maximized  $\square_4$  (see main text for details), here  $t_1 = 820.1 s$  and  $t_2 = 1451.7 s$  for repulsive glass and attractive glass, respectively.

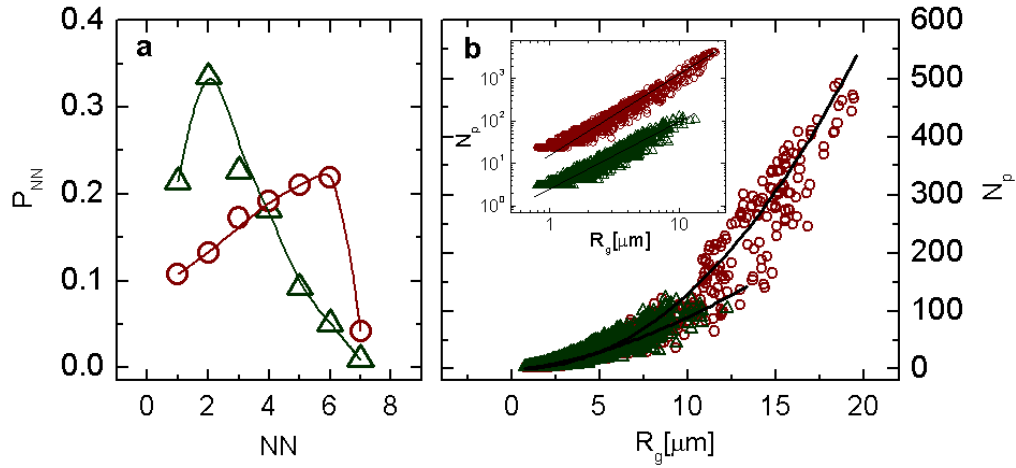


**FIG. 4.** Size and shape of CRR clusters in attractive and repulsive glasses. (a) Distribution of the number of nearest neighbors in CRR clusters,  $P_{NN}$ , versus the number of nearest neighbors,  $NN$ , for repulsive glass (triangles) and attractive glass (circles). Particles in CRRs of repulsive glasses and attractive glass have an average of  $2.5 \pm 1.0$  (mean, standard deviation) nearest neighbors and  $4.4 \pm 1.2$  nearest neighbors, respectively. The lines are guides for the eye. (b) Number of particles in a cluster,  $N_p$ , as a function of cluster radius of gyration,  $R_g$ . Triangles and circles denote repulsive glass and attractive glass, respectively. Lines are power-law fits that enable us to extract the fractal dimension associated with the CRRs. Inset: Same data on a log-log plot. For clarity, data for attractive glass in the inset are multiplied by ten in vertical axis.